The *Arabidopsis* flagellin receptor FLS2 mediates the perception of *Xanthomonas* Ax21 secreted peptides

Cristian H. Danna[a,b], Yves A. Millet[a,b], Teresa Koller[c], Sang-Wook Han[d], Andrew F. Bent[c], Pamela C. Ronald[d], and Frederick M. Ausubel[a,b,1]

[a]Department of Genetics, Harvard Medical School, Boston, MA 02114; [b]Department of Molecular Biology, Massachusetts General Hospital, Boston, MA 02114; [c]Department of Plant Pathology, University of Wisconsin, Madison, WI 53706; and [d]Department of Plant Pathology, University of California, Davis, CA 95616

Contributed by Frederick M. Ausubel, April 20, 2011 (sent for review April 5, 2011)

Detection of microbes by plants relies in part on an array of pattern-recognition receptors that recognize conserved microbial signatures, so-called "microbe-associated molecular patterns." The *Arabidopsis thaliana* receptor-like kinase FLS2 is the pattern-recognition receptor for bacterial flagellin. Similarly to FLS2, the rice transmembrane protein XA21 is the receptor for the sulfated form of the *Xanthomonas oryzae* pv. *oryzae* secreted protein Ax21. Here we show that Ax21-derived peptides activate *Arabidopsis* immunity, triggering responses similar to those elicited by flagellin, including an oxidative burst, induction of defense-response genes, and enhanced resistance to bacterial pathogens. To identify *Arabidopsis Xa21* functional homologs, we used a reverse genetics approach to screen T-DNA insertion mutants corresponding to all 47 of the *Arabidopsis* genes encoding non-RD kinases belonging to the interleukin-1 receptor-associated kinase (IRAK) family. Surprisingly, among all of these mutant lines, only *fls2* mutants exhibited a significant loss of response to Ax21-derived peptides. Ax21 peptides also failed to activate defense-related responses in an *fls2-24* mutant that does not bind Flg22. Moreover, a Flg22Δ2 variant of Flg22 that binds to FLS2 but does not activate FLS2-mediated signaling suppressed Ax21-derived peptide signaling, indicating mutually exclusive perception of Flg22 or Ax21 peptides by FLS2. The data indicate that FLS2 functions beyond flagellin perception to detect other microbe-associated molecular patterns.

innate immunity | broad spectrum MAMP recognition | non-RD kinases

Pattern-recognition receptors (PRRs) that recognize conserved microbial signatures, which are referred to as microbe-associated molecular patterns (MAMPs), are a key mechanism by which plants and other organisms detect microbes (1). Among several MAMPs detected by *Arabidopsis thaliana*, flagellin is the best studied. In *Arabidopsis*, the leucine-rich repeat (LRR) transmembrane receptor kinase FLAGELLIN SENSITIVE 2 (FLS2) is essential for flagellin perception (2). A 22-aa synthetic peptide (Flg22) corresponding to the recognized domain of flagellin activates FLS2-dependent signaling, triggering the same responses as the native flagellin protein from *Pseudomonas syringae* pv. *tabaci* (3). Flg22-triggered responses include activation of MAPK cascades, up-regulation of defense genes, transient production of an H_2O_2 oxidative burst, deposition of callose, and enhanced resistance against pathogens (2, 4, 5).

The *Arabidopsis* FLS2 receptor belongs to the IRAK family of receptor like kinases (RLKs), which includes two other well characterized MAMP receptors, *Arabidopsis* EFR (TU-elongation factor-receptor 1) and rice XA21 (*Xanthomonas* resistance protein 21) (6). These RLKs carry the non-RD domain, a motif that is found in many IRAK kinases that function in immune signaling pathways (6). The *Arabidopsis* genome encodes 47 non-RD IRAK kinases, of which 35 are RLKs and 12 are predicted to be cytoplasmic (6, 7).

XA21 recognizes the conserved *Xanthomonas oryzae* pv. *oryzae* (*Xoo*) Ax21 secreted protein (8). Rice plants carrying the *Xa21* gene are fully resistant to *Xoo* carrying Ax21. A synthetic sulfated 17-aa peptide (axY^{S}22) derived from Ax21 (residues 17–33 of the Ax21 protein) binds XA21 and triggers enhanced resistance against *Xoo*. Replacing sulfated Tyr (at amino acid position 22 of Ax21) by Ala abolishes Ax21 perception, indicating that the sulfated Tyr residue is required for activity (9).

Here we present data showing that Ax21-derived peptides are also recognized by *Arabidopsis*, and surprisingly, that this recognition is mediated by FLS2, which was previously thought to be highly specific for flagellin. If individual MAMP receptors are capable of recognizing a variety of MAMPs, it increases the spectrum of microbe-derived molecules that can activate an immune response using a relatively limited number of PRRs.

Results

Ax21-Derived Peptides Are Perceived by *Arabidopsis*. Because Ax21 is conserved among *Xanthomonas* species, including *Xanthomonas campestris campestris* (*Xcc*), which is an *Arabidopsis* pathogen, we hypothesized that *Arabidopsis* may be able to respond to Ax21 similarly to other well-characterized MAMPs. Although supernatant extracts from *Xcc* do not normally elicit rice XA21-mediated immunity, they do when a plasmid containing the putative sulfotransferase *RaxST* from *Xoo* is introduced into the otherwise unrecognized *Xcc* bacterial strain (10), suggesting that the examined *Xcc* strains have the capability of normally secreting nonsulfated Ax21. Bacterial extracts from an isogenic Xcc Δ*fliC* mutant expressing a variant of flagellin that is not perceived by *Arabidopsis*, still triggered MAMP responses similar to wild-type *Xcc*, indicating that other MAMPs from *Xcc* besides flagellin are recognized by *Arabidopsis* (11), one of them potentially being Ax21.

To test whether Ax21-derived peptides are perceived by *Arabidopsis*, we infiltrated axY22, the nonsulfated version of the sulfated 17-aa peptide recognized by rice, into wild-type Col-0 plants carrying either *WRKY11p::GUS* or *MYB51p::GUS* reporter constructs. These two promoter-reporter constructs were previously shown to be activated by a variety of MAMPs, including Flg22 and Elf26 (a synthetic 26-aa peptide corresponding to elongation factor EF-Tu) (12). Indeed, infiltration of 1 μM axY22 triggered activation of *WRKY11p::GUS* and *MYB51p::GUS* similar to 1 μM Flg22 (Fig. 1). Surprisingly, the sulfated version of axY22 (axY^{S}22), as well as a derivative of axY^{S}22 that is unable to trigger XA21-mediated immunity, axY22A, which contains alanine instead of tyrosine at position 22 (9), also activated the *Arabidopsis* MAMP reporters (Fig. 1).

Treatment of plants with MAMPs has been shown to trigger a complex and multilayered defense response, including elicitation of a transient H_2O_2 burst (2). To facilitate the study of Ax21 perception in *Arabidopsis*, we developed a miniaturized and

---

Author contributions: C.H.D., S.-W.H., P.C.R., and F.M.A. designed research; C.H.D., Y.A.M., and T.K. performed research; C.H.D., Y.A.M., T.K., S.-W.H., A.F.B., P.C.R., and F.M.A. analyzed data; and C.H.D. and F.M.A. wrote the paper.

The authors declare no conflict of interest.

[1]To whom correspondence should be addressed. E-mail: ausubel@molbio.mgh.harvard.edu.

This article contains supporting information online at www.pnas.org/lookup/suppl/doi:10.1073/pnas.1106366108/-/DCSupplemental.

www.pnas.org/cgi/doi/10.1073/pnas.1106366108

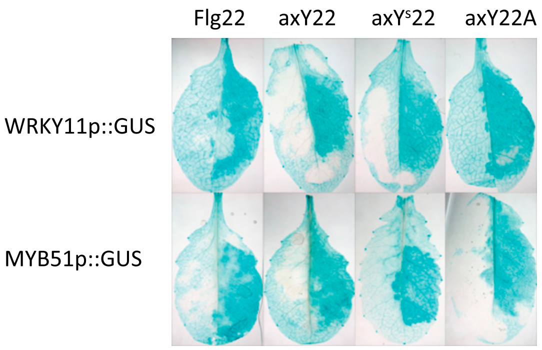

Fig. 1. Ax21-derived peptides trigger MAMP-responsive gene expression in *Arabidopsis*. Leaves from 6-wk-old Col-0 transgenic plants carrying *WRKY11::GUS* or *MYB51::GUS* constructs were infiltrated with 1 μM peptides (*Right*) or water (*Left*) and stained with GUS, as described in *SI Methods*.

relatively high throughput assay to measure H_2O_2 bursts in 10-d-old seedlings germinated in liquid MS medium in 96-well assay plates. In agreement with the results shown in Fig. 1, peptides previously shown to be either active (axY^{s}22) or inactive (axY22, axY22A) in rice elicited an H_2O_2 burst in *Arabidopsis* (Fig. 2). However, in contrast to adult *Arabidopsis* plants, where relatively low concentrations of Ax21 peptides (1 μM) were sufficient to trigger reporter gene expression (Fig. 1), significantly higher concentrations (∼100 μM) of the Ax21 peptides were necessary to elicit H_2O_2 production in seedlings. The effective concentration Ax21 peptides that arise at sites of bacterial infection are not known, but concentrations of exogenously applied axY^{s}22 peptide in the range of 1–100 μM are also necessary to trigger immunity in rice (9).

To determine whether the recognition of Ax21 peptides by *Arabidopsis* results in a biologically significant response, we tested whether Ax21-derived peptides trigger enhanced resistance in seedlings to *P. syringae*, similarly to Flg22-elicited protection of seedlings against *P. syringae* (13). By using a *P. syringae* pv. *maculicola* (*Psm*) strain expressing the *LUX* operon from *Photorhabdus luminescens*, we were able to monitor bacterial growth by measuring light emission in a scintillation counter (adapted from refs. 13 and 14). For this MAMP-elicited protection assay, seedlings were grown in 12-well plates (20–30 seedlings per well) for 10 d and elicited with various MAMPs, including Ax21 peptides, for a period of 24 h before inoculation with *Psm*-LUX. To assess bacterial growth inside seedlings, washed seedlings were ground at different times after inoculation and luminescence was measured with a scintillation counter. Bacterial growth was estimated by converting light emission into CFUs (using an experimentally determined CPMs/CFUs conversion table). Although relatively high concentrations of the Ax21 peptides were necessary to detect protection activity (100 μM), as in the case of the oxidative burst (Fig. 2), peptides that are either active (axY^{s}22) or inactive (axY22 and axY22A) in rice were equally capable of triggering enhanced resistance against *P. syringae* in *Arabidopsis* (Fig. 3*A*). Similarly to the concentration of Flg22 required to elicit an oxidative burst in the seedling assay, 1 μM Flg22, but not lower concentrations, elicited protection against *Psm*-LUX. Importantly, both Flg22 and axY^{s}22 peptides also elicited enhanced resistance against *X. campestris* (Fig. 3*B*), which suggests that perception of Ax21-derived peptides could be part of a natural *Arabidopsis* defense mechanism against *Xcc*.

In an effort to determine which amino acids in the 17-aa synthetic axY^{s}22 peptide are important for perception by *Arabidopsis*, we tested a previously described collection of 17 peptides, each one carrying an alanine in place of the original amino

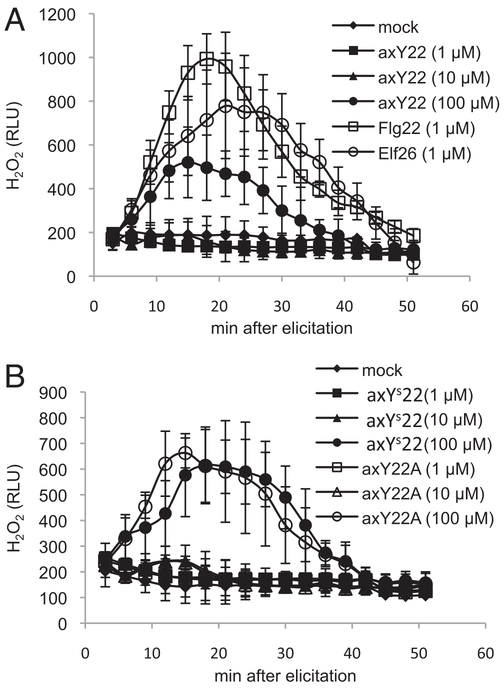

Fig. 2. Ax21-derived peptides trigger a hydrogen peroxide burst. Ten-day-old Col-0 wild-type seedlings were grown in 96-well plates and mock-treated or elicited with axY22, Flg22, or Elf26 (*A*) or with axY^{s}22 or axY22A (*B*) at the indicated concentrations: axY^{s}22 is the sulfated 17-mer that is active in rice; axY22 is the nonsulfated version of axY^{s}22; axY22A contains a Tyr→Ala substitution. Neither axY22 nor axY22A can trigger rice XA21-mediated immunity. Each point represents the mean of six seedlings. Error bars represent ± SD of the mean. Essentially identical results were obtained in at least three independent experiments.

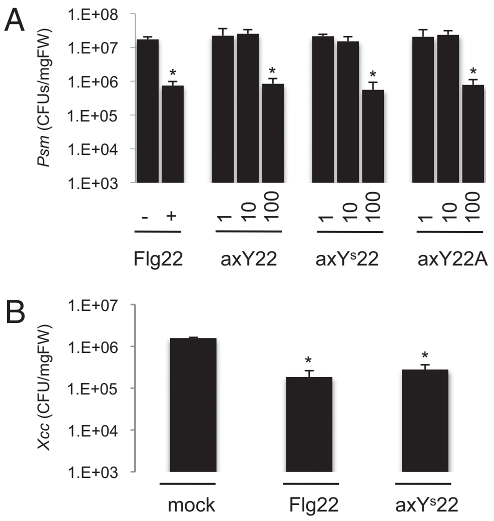

Fig. 3. Ax21-derived peptides trigger enhanced resistance against bacteria. (*A*) Ten-d-old seedlings were grown in 12-well plates, elicited with 1 μM Flg22 or 1 μM, 10 μM, or 100 μM axY22, axY^{s}22, or axY22A for 24 h, and then infected with *Psm-LUX*. Bacterial titer was assessed as CFU/mg fresh weight seedling tissue 36 h after inoculation: axY^{s}22 is the sulfated 17-mer that is active in rice; axY22 is the nonsulfated version of axY^{s}22; axY22A contains a Tyr→Ala substitution. Neither axY22 nor axY22A can trigger rice XA21-mediated immunity. (*B*) Seedlings were elicited with 100 μM axY^{s}22 for 24 h and then inoculated with *Xcc*. Each column represents the bacterial titer 24 h after inoculation as CFU/mg fresh weight seedling tissue and is the mean of three wells containing 20 seedlings each. Error bars represent ± SD of the mean. Essentially identical results were obtained in at least three independent experiments. *$P < 0.001$ compared with mock (*t* test).

acid, except for residue #1 (which normally contains an Ala at that position) that was replaced by Gly (9). Surprisingly, all of these modified peptides exhibited a similar level of activity as axY22 or axY^{s}22 in the *P. syringae* protection assay when tested at 100 μM (Fig. S1*A*). However, replacing Ala by Gly at position #1 (axY^{s}22-A1), or Glu by Ala at position #2 (axY^{s}22-A2), increased the activity of the peptide by at least 10-fold (Fig. S1 *B* and *C*). That is, the two peptides containing substitutions at one of the two N-terminal residues were as active at 10 μM as axY22 or axY^{s}22 were at 100 μM.

One explanation for the unexpected result that all of the substituted Ax21 peptides had activity at 100 μM is that all peptides at such a relatively high concentration would nonspecifically elicit a robust defense response or would directly inhibit the growth of *P. syringae*. To test this possibility, we pretreated seedlings with high concentrations of peptides that have been reported to be inactive in *Arabidopsis*. A Flg22-like peptide derived from *Agrobacterium tumefaciens* (Flg22$^{A.tum}$), or a Flg22-derived peptide Flg22Δ2, both previously shown to be inactive in adult *Arabidopsis* plants (15), were also inactive at 100 μM in the seedling protection assay (Fig. S2), suggesting that a high concentration of any peptide does not trigger nonspecific activation of MAMP-elicited responses. To further test the specificity of peptide perception in seedlings, we tested Flg22 and Elf26 perception in *fls2* and *efr* receptor mutants, respectively. High concentrations of active Flg22 or active Elf26 did not trigger a measurable response in the corresponding receptor mutants (Fig. S3), suggesting that high concentrations of peptides do not bypass the requirement for a specific receptor. Finally, to further assess whether the Ax21 peptide response is receptor-specific, we performed a saturation experiment with the axY^{s}22 peptide. We found that at concentrations greater than 100 μM of peptide the response was saturated, indicating that Ax21 perception is most likely mediated by a specific receptor or receptors (Fig. S4).

Because the axY^{s}22-A1 peptide is 10-fold more active than the wild-type peptide in the *Arabidopsis* assays described in this section, we used 10 μM axY^{s}22-A1 for most of the experiments described below.

FLS2 Is Required for Perception of Ax21-Derived Peptides. Most of the known MAMP receptors in plants, including FLS2, EFR, and rice XA21, belong to the IRAK family of non-RD kinases. In an effort to identify *Arabidopsis* Ax21 peptide receptor(s), we used the axYs22-A1 peptide in the seedling oxidative burst and protection assays to test a collection of 71 mutant lines consisting of one or two (when available) T-DNA insertion mutations corresponding to each of the 47 non-RD IRAK kinase genes. Surprisingly, only two independent T-DNA insertions in the *fls2* gene compromised the H_2O_2 burst (Fig. 4*A*) or the protection against *P. syringae* (Fig. 4*B*) after axY^{s}22-A1 elicitation (Table S1). Similar results were obtained with these two *fls2* mutants in larger scale assays in 12-well plates, where the two *fls2* mutants also failed to respond to axY^{s}22-A1, axY^{s}22 or axY22 (Fig. 4*C*).

Ax21 Peptides Elicit the Same Responses as Flagellin. To further characterize FLS2-mediated perception of axY^{s}22-A1, we tested whether the NADPH oxidase RBOHD (respiratory burst oxidase homolog D), an enzyme that has been shown to be required for reactive oxygen species production after elicitation with Flg22 (16), is also necessary for the axY^{s}22-A1 triggered H_2O_2 burst. Indeed, an *AtrbohD* mutant did not exhibit an H_2O_2 burst following treatment with axY^{s}22-A1 (Fig. 5*A*). Moreover, we found that mutations in the FLS2 adaptor protein BAK1, which is required for Flg22-elicited signaling (17), partially compromised the enhanced resistance triggered by axY^{s}22-A1 (Fig. 5*B*). Finally, we found that in the seedling assay, 5 μM axY^{s}22-A1 activates the expression of a set of genes previously shown to be up-regulated by 1 μM Flg22 (18) in an FLS2-dependent manner (Fig. 5*C*). These data show that axY^{s}22-A1 triggers a similar cascade of downstream events as those triggered by Flg22, which is consistent with the hypothesis that FLS2 is the axY^{s}22-A1 receptor.

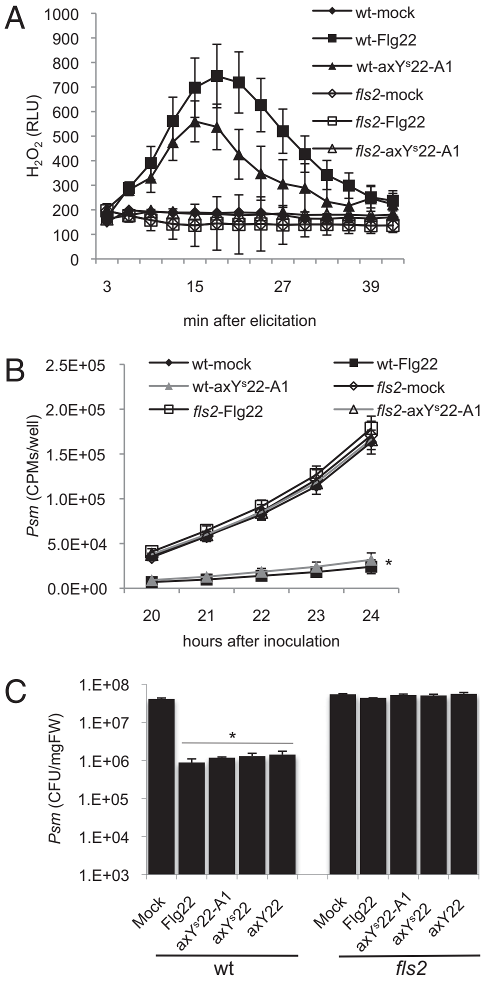

Fig. 4. FLS2 is necessary for Ax21-derived peptide perception. (*A*) A hydrogen peroxide burst was elicited in 10-d-old Col-0 wild-type or *fls2* mutant (SAIL_691_C04) seedlings in 96-well plates with axY^{s}22-A1 (10 μM) or Flg22 (1 μM). Each datapoint represents the mean of six seedlings (six wells). Error bars represent ± SD of the mean. (*B*) Ten-d-old Col-0 wild-type or *fls2* (SAIL_691_C04) seedlings were grown in 96-well plates, elicited with axY^{s}22-A1 (10 μM) or Flg22 (1 μM) for 24 h and then infected with *Psm-LUX*. Bacterial titer was determined with a 96-well plate scintillation counter each hour between 20 and 24 h after inoculation. Each datapoint represents the mean of six seedlings (six wells). Error bars represent ± SD of the mean. (*C*) Ten-day-old Col-0 wild-type or *fls2* mutant (SAIL_691_C04) seedlings were grown in 12-well plates and elicited with various Ax21 peptides and infected with *Psm-LUX* as in Fig. 3*A*. A second *fls2* insertion mutant (Salk_121477) showed identical results. Each column represents the mean of three wells containing 20 seedlings each. Error bars represent ± SD of the mean. Essentially identical results were obtained in at least three independent experiments. *$P < 0.001$ compared with mock (*t* test).

Flg22 Binding Domain of FLS2 Is also Required for Ax21 Peptide Activity. The FLS2 receptor is a 1,173-aa protein that consists of an intracellular kinase domain, a hydrophobic membrane-spanning domain, and an extracellular domain composed of 25 LRRs (19). A single nucleotide change in LRR #10 (G → R 318, referred to as the *fls2-24* allele) abolishes the binding of Flg22 without compromising the accumulation or stability of FLS2 protein (15, 20), as do other nearby mutations in the proposed binding domain for Flg22 (21). To initiate studies to determine whether Flg22 and axY^{s}22-A1 use the same binding domain to activate

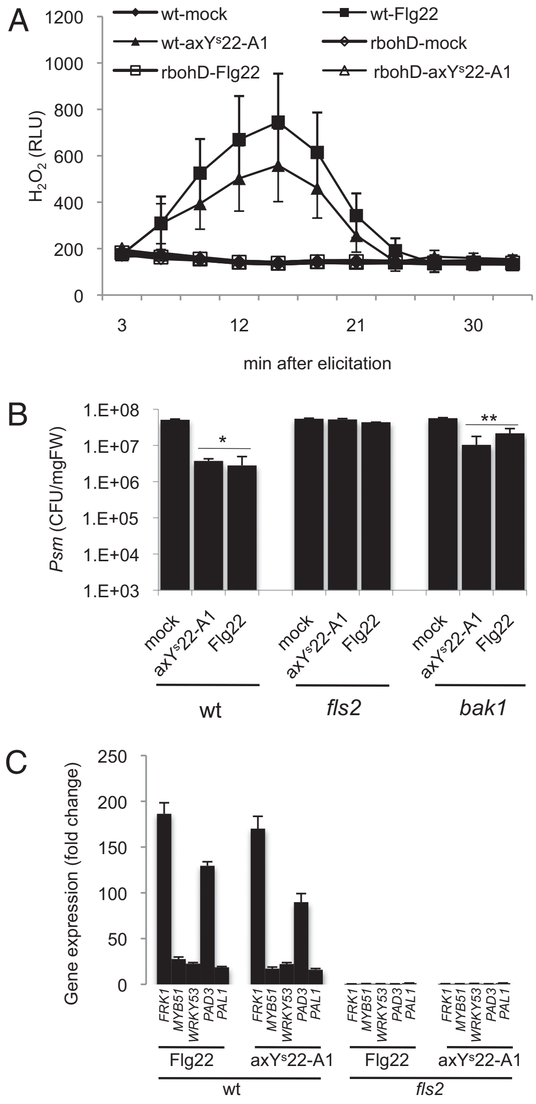

Fig. 5. FLS2-mediated perception of Ax21-derived peptides mimics Flg22 perception. (*A*) A hydrogen peroxide burst was elicited in 10-d-old Col-0 wild-type or *AtrbohD* mutant seedlings with axY^{s}22-A1 (10 μM) or Flg22 (1 μM) in 96-well plates. Each datapoint represents the mean of six seedlings (six wells). Error bars represent ± SD of the mean. (*B*) Ten-d-old Col-0 wild-type, *fls2* mutant (SAIL_691_C04), or *bak1* mutant (SALK_116202) seedlings were grown in 12-well plates and elicited with axY^{s}22-A1 (10 μM) or Flg22 (1 μM) and then infected with *Psm-LUX* as in Fig. 3*A*. Columns represent the mean of three wells containing 20 seedlings each. Error bars represent ± SD of the mean. (*C*) Ten-day-old Col-0 wild-type or *fls2* mutant seedlings were grown in 12-well plates and elicited with Flg22 (1 μM) or axY^{s}22-A1 (5 μM) for 3 h. RNA was extracted and qRT-PCR analysis was carried out as described in *SI Methods*. Gene expression is shown as fold-change compared with mock treatment. Columns represent the mean of three independent qRT-PCR reactions. Error bars represent ± SEM. Essentially identical results were obtained in at least three independent experiments. $^*P < 0.001$ and $^{**}P < 0.01$ compared with mock (*t* test).

FLS2, we tested the *fls2-24* mutant for H_2O_2 production after elicitation with axY^{s}22-A1 peptide. The *fls2-24* mutant did not exhibit an H_2O_2 burst after axY^{s}22-A1 elicitation (Fig. 6*A*). To further test the hypothesis that Flg22 and axY^{s}22-A1 share a binding site on FLS2, we performed competition experiments between axY^{s}22-A1 and Flg22Δ2, a Flg22-derived peptide that has been shown to compete with Flg22 by binding to the FLS2 receptor but not triggering FLS2 activation (15). The addition of Flg22Δ2 at the same concentration as axY^{s}22-A1 strongly reduced the H_2O_2 burst triggered by axY^{s}22-A1 (Fig. 6*B*), whereas a 10-fold molar excess of Flg22Δ2 was necessary to partially inhibit the Flg22-triggered H_2O_2 burst (Fig. S5*A*). As a control, a 10-fold molar excess of Flg22Δ2 did not have any measurable effect on the Elf26-triggered H_2O_2 burst (Fig. S5*B*). Although competition through binding at separate sites is possible, the simplest explanation for Flg22Δ2 suppression of both Flg22- and axY^{S}22-A1-mediated signaling is competition for the same binding domain on FLS2.

Synthetic Peptide axY^{s}22-A1 Is Not Contaminated with Flg22. To rule out the possibility of contamination of the axY^{S}22-A1 stock solution with Flg22, we analyzed axY^{s}22-A1 by mass spectrometry (Fig. S6). We did not detect any contaminants at the concentration used in our assays (10 μM). In particular, Flg22 with a detection limit of 10 nM (Fig. S6) was not present in the stock. Because concentrations of Flg22 below 1 μM are insufficient to trigger protection against *Psm*-LUX or to elicit an oxidative burst in *Arabidopsis* seedlings in our assay, these results make it extremely unlikely that Flg22 contamination of the axY^{s}22-A1 stock solution would explain FLS2-dependent axY^{s}22-A1 peptide perception.

Discussion

Plant defense against microbial attack uses a limited number of preformed receptors that recognize pathogen-related signature molecules. MAMP receptors, such as the *Arabidopsis* receptor kinases FLS2 and EFR, recognize highly conserved pattern molecules, such as flagellin and elongation factor EF-Tu, respectively. If plants had promiscuous MAMP receptors that were able to recognize multiple MAMPs, it would expand the variety of

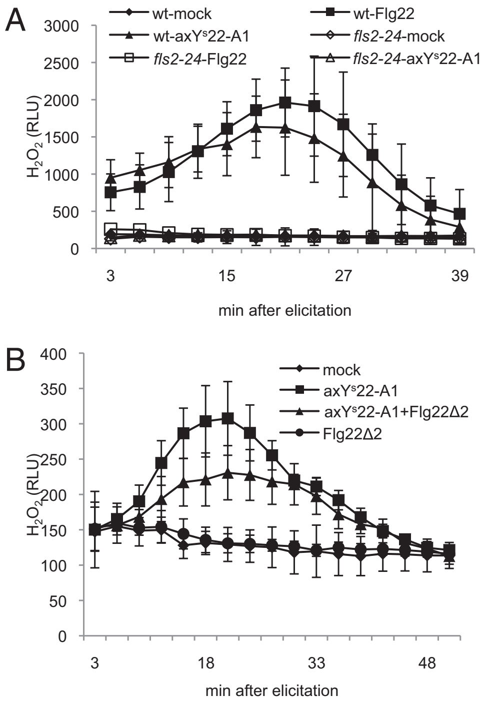

Fig. 6. The Flg22 binding domain of FLS2 is also required for Ax21-derived peptide perception. (*A*) A hydrogen peroxide burst was monitored in 10-d-old L*er* wild-type or *fls2-24* mutant seedlings in 96-well plates after elicitation with Flg22 (1 μM) or axY^{s}22-A1 (10 μM). (*B*) A hydrogen peroxide burst was monitored in Col-0 wild-type seedlings after elicitation with axY^{s}22-A1, Flg22Δ2, or a combination of both peptides. Each datapoint represents the mean of six seedlings (six wells). Error bars represent ± SD of the mean. Essentially identical results were obtained in at least three independent experiments (*A*) or two independent experiments (*B*).

MAMPs that an individual plant could recognize without devoting a large fraction of the genome to PRRs. In addition, because MAMPs are likely to be present in low concentrations in a natural infection, the simultaneous recognition of multiple MAMPs may help to strengthen MAMP-mediated signaling. The promiscuity of FLS2 in recognizing both flagellin and the Ax21-derived peptides produced by *Xanthomonas* suggests that the *Arabidopsis* immune system has evolved to maximize the utility of a limited number of PRRs.

MAMP recognition in mammals is carried out by Toll-like receptors (TLRs), transmembrane receptors with LRR external domains, and associated non-RD cytoplasmic kinases, which together are functionally equivalent to FLS2 or XA21. The mammalian receptor TLR2 was initially thought to bind MAMPs as different in structure as LPS, peptidoglycan, and lipoproteins from diverse bacteria and parasites. Later studies, however, demonstrated that LPS and peptidoglycan preparations were contaminated with lipoproteins or lipopeptides (22), which are now thought to be the actual ligands of TLR2. Because all of the peptides used in our study were synthetic (HPLC-purified and subjected to mass spectrometry to confirm mass and sequence and potential contamination with Flg22) (Fig. S6), the apparent promiscuity of FLS2 that we observe cannot be explained as an artifact caused by flagellin or Flg22 contamination.

Mammalian TLR receptors, such as TLR2 and TLR6, can form heterodimers, which broaden the range of specificity of these receptors. TLR2-TLR6 heterodimers recognize 2-acyl-lipoproteins, whereas TLR6 homodimers recognize lipoteicoic acid and zymosan and TLR2 homodimers seem to be inactive (23). A similar mechanism may operate in plants and is a viable hypothesis for the apparent promiscuity of FLS2, although partner MAMP receptors for FLS2 have not been identified. Alternatively, because Flg22 and Ax21 peptides do not show any obvious sequence similarity, it is possible that FLS2 may function as a coreceptor for another protein that is the actual receptor for the Ax21-derived peptides. Consistent with the idea that MAMP receptors function in complexes with transmembrane receptor partners, FLS2 and EFR function in concert with the coreceptor kinase BAK1, which is also required for BRI1-mediated perception of brassinolide (17, 24). However, there is no evidence that BAK1 interacts directly with brassinolide or MAMPs.

In contrast to the coreceptor model, our data suggest that the Flg22- and Ax21-dervived peptides directly bind to FLS2 because an FLS2 mutation that affects the binding of Flg22 to FLS2 blocked Ax21-derived peptide elicited responses (Fig. 6*A*). Furthermore, a deleted version of Flg22, Flg22Δ2, which functions as a suppressor of Flg22 responses (15), partially suppressed the axY^{S}22-A1–mediated oxidative burst (Fig. 6*B*), again suggesting that Flg22- and Ax21-derived peptides may compete for the same binding site on FLS2 (Fig. 6*B*). Whether FLS2 is the only receptor for Ax21-derived peptides or whether FLS2 is recruited in a receptor complex together with other receptors and adaptors that may modulate its specificity, remains to be determined.

If FLS2 is not the direct or the only receptor providing the binding site for Ax21 peptides, it is unlikely than any of the other 34 *Arabidopsis* non-RD RLKs function as an Ax21 peptide receptor, because T-DNA insertions in the corresponding genes do not affect the ability of Ax21 peptides to activate an *Arabidopsis* immune response, unless they have redundant functions in partnering with FLS2 for Ax21 perception. We limited our search for potential Ax21 receptors to those with the non-RD types of kinase domain (Table S1) because genomic analysis indicated that the presence of the non-RD motif is highly predictive of a function in the innate immune response in both plants and animals (6). For example, all plant non-RD kinases that have been assigned a physiological function serve a key role in innate immunity, including three of the best-studied plant PRRs, FLS2, EFR, and XA21. Because XA21 is closely related to *Arabidopsis* non-RD RLKs of the subfamily LRR-XII, which includes FLS2 and EFR (6, 25), the identification of *AtFLS2* as an *Xa21* functional homolog is perhaps somewhat predictable. Nevertheless, because the extracellular LRRs of FLS2 and XA21 have no compelling similarity and FLS2 was thought to be specific for flagellin perception, the result that perception of Ax21-derived peptides requires FLS2 is striking.

Given the significant level of identity between FLS2 and XA21, and in light of our data suggesting that FLS2 may be the receptor for Ax21-derived peptides, it is interesting to note that rice cultivars that lack *Xa21* but that still encode functional OsFLS2 do not respond to Ax21-expressing *Xanthomonas* strains (8) and do not perceive Ax21 peptides (9). These latter data suggest that OsFLS2 does not have the broad ligand specificity exhibited by AtFLS2, or that the experimental protocols used in the rice experiments were not sensitive enough to detect this broad specificity.

One explanation for the current divergent specificities of OsFLS2 and AtFLS2 is to postulate the existence of an ancient progenitor of OsFLS2 and AtFLS2 that had the broad ligand specificity of AtFLS2. In the *Arabidopsis* lineage, a broad ligand-specificity of the ancient receptor may have been preserved, but in the rice lineage, a gene duplication may have allowed one paralog (*FLS2*) to lose its capacity to perceive Ax21 peptides as the other paralog (*Xa21*) evolved a high level of specificity for sulfated Ax21 peptides in the wild species *Oryza longistaminata*. One line of evidence in support of this model is that AtFLS2 recognizes many different variants of the axY^{S}22 17-mer in addition to Flg22 (Figs. 1 and 2, and Fig. S1). This proposed evolutionary course of events makes sense in light of the vast expansion of predicted PRRs in rice compared with dicots. With nearly 10-fold fewer predicted PRRs, [328 non-RD RLKs in rice versus 35 in *Arabidopsis* (1, 7)], *Arabidopsis* PRRs need to have broad specificity to detect as many MAMPs as rice.

Although microbes can potentially produce a very large number of conserved signatures, only a few MAMPs have been identified, and most of these trigger a similar set of responses. MAMP responses include alkalinization of the apoplast, transcriptional up-regulation of defense genes, activation of MAP kinases, deposition of callose, and the transient production of reactive oxygen species (oxidative burst). It is not known, however, if these responses are universal. We therefore suggest that the assessment of MAMP-enhanced resistance, which is likely to be the ultimate consequence of MAMP recognition, may be the most appropriate way to assess MAMP perception. In this article, we describe the development of a high throughput assay for detecting enhanced resistance against bacterial infection (Fig. 4*B*), which may assist in the identification of novel MAMPs.

The lack of physical information to conclusively define the ligand binding sites of FLS2 makes it difficult to understand how a single receptor mediates the perception of MAMPs with no apparent structural similarity. However, in light of our functional data showing that FLS2 mediates perception not only of flagellin but also of Ax21-derived peptides, it is possible that FLS2 (as well as XA21 and other PRRs) may mediate recognition of other ligands as well. Hence priorities for future research include not only identification of the binding sites of known ligands for well-characterized PRRs, but also discovery of additional putative ligands and potential partner proteins that may alter plant PRR extracellular domain configuration and ligand specificity.

Methods

Plant Growth. Adult plants were grown in climate-controlled growth rooms (Conviron MTPS144) on Metro-Mix 360 soil (Sun Agro) at 22 °C, 75% humidity, and a 16 h photoperiod at 100 $\mu E \cdot m^{-2} \cdot s^{-1}$ of light (for genotyping of T-DNA lines and seed propagation) or a 12-h photoperiod (for GUS staining). SALK_ and SAIL_ T-DNA insertion lines were obtained from the Arabidopsis Biological Resource Center (http://abrc.osu.edu/). GABI_Kat lines were obtained from the Arabidopsis Biological Resource Center or from NASC (http://arabidopsis.info/). An *Arabidopsis atrbohD* mutant was obtained from M. A. Torres (Universidad Politécnica de Madrid, Spain). The *fls2-24* mutant was obtained from T. Boller (Botanical Institute, University of Basel, Switzerland). Genotyping was carried out by PCR of genomic DNA using PCR primers designed by SIGnal T-DNA Express and following the recommended combination of primers (http://signal.salk.edu/tdnaprimers.2.html). A complete list of PCR primers is shown in Table S2. For detailed information on genotyping see *SI Methods*.

Seedling Liquid Culture. For growing seedlings in liquid medium in 12-well assay plates (BD Falcon; 353043), seeds were sterilized in 20% bleach (2 min), washed three times with sterile water, and 20 to 30 seeds were dispensed into wells containing 1 mL MS 1× medium (Murashige and Skoog basal medium with vitamins from Phytotechnology Laboratories supplemented with 0.5 g/L Mes hydrate and 0.5% sucrose at pH 5.7). Seedlings were grown for 10 d (replacing medium at day 8) at 22 °C, 95% humidity (to prevent medium evaporation) in a plant growth chamber (Conviron; E7/2) under 100 $\mu E \cdot m^{-2} \cdot s^{-1}$ and a 16-h photoperiod.

For growing seedlings in 96-well plates (Greiner Bio-One; 655083), seeds were sterilized as above and several seeds were dispensed into each well containing 125 μL MS 1× medium (see above). At day 8, the medium was replaced using an eight-well vacuum manifold connected to a vacuum line and seedlings were thinned to leave a single seedling per well. Seedlings were grown for 2 more days at 22 °C, 95% humidity in a plant growth chamber (Conviron; E7/2) under 100 $\mu E \cdot m^{-2} \cdot s^{-1}$ and a 16-h photoperiod.

Synthetic Peptides. Flg22, Flg22$^{\mathrm{A.tum}}$, Flg22Δ2 and Elf26 were synthesized by the Massachusetts General Hospital-Peptide/Protein Core Facility. Ax21-derived peptides were synthesized by Pacific Immunology Corporation. For a complete list of Ax21-derived peptides, see ref. 9. Lyophilized peptides were resuspended in sterile water. Mass spectrometry was used to determine the purity of the axY^{s}22-A1 peptide as described in *SI Methods* and Fig. S6.

Luminol Chemiluminescence Assay for H_2O_2 Detection in 96-Well Plates. Ten-day-old seedlings were removed from the growth chamber 4 h after the beginning of the light period and kept in the dark for 30 min before elicitation. For the rest of the assay, plates were kept in the dark. Every plate contained 12 wells containing Col-0 wild-type seedlings in row A. Each plate also contained seven different T-DNA insertion lines in rows B to H, (12 seedlings per row; 1 seedling per well). In columns 1 to 6, seedlings were treated with water. In columns 7 to 12, seedlings were treated with peptides (10 μL, in water). A second plate containing the same distribution of wild-type and T-DNA lines was elicited with peptides (10 μL) in columns 1 to 6 and water in columns 7 to 12. After the addition of 10 μL of water or peptides, plates were centrifuged briefly at 30 × *g* (Beckman Coulter Allegra ×22 swinging arms centrifuge) to ensure that the added peptides were distributed into the medium and that seedlings were exposed to peptide. Immediately after centrifugation, 10 μL of a Luminol-HRP solution in 100 mM K_2/KPO_4 buffer pH 7.9 [0.5 μg/mL Luminol (A4685) plus 0.5 μg/mL Type VI-A HRP from Sigma (P6782)] was added to each well and the plates were briefly centrifuged again. Plates were placed into the 96-well scintillation reader and light emission was monitored using a 96-well scintillation counter (1450 Microbeta Wallac TriLux Scintillation/Luminescence counter). Every well was read for a total of 5 s in noncoincidental mode. Every plate was read in full 20 to 25 times (every 2.5 min) for a total of 40 to 50 min. Kinetics of H_2O_2 production were determined by integration of data for every well over the reading period. Every time point is the mean value of six seedlings (either mock or peptide elicited).

MAMP-Triggered Enhanced Resistance Assay in 96-Well Plates. Ten-day-old seedlings in 96-well assay plates were grown and arranged in the assay plates and either mock-treated or elicited with peptides as described above for the oxidative burst assays. Seedlings were grown for an additional 24 h after the peptide or mock treatment and then inoculated with 10 μL of *P. syringae* pv. *maculicola* strain ES4326 (OD_{600} = 0.0002) carrying the LUX operon from *P. luminescens* (*Psm-LUX*) (14). Bacterial growth was carried out as indicated in *SI Methods*. Inoculated seedlings were grown for 20 h and then transferred hourly to the 96-well scintillation counter for light quantification, as described above. Reads were repeated every hour for a total of 6 h. Kinetics of bacterial growth was determined by integration of data for each well. Each time point is the mean value of six seedlings (either mock or peptide elicited).

MAMP-Triggered Enhanced Resistance Assay in 12-Well Plates. Ten-day-old seedlings, germinated and grown in 12-well plates, as described above, were mock-treated with water or treated with peptides for 24 h, inoculated with 100 μL of *Psm-LUX* (OD_{600} = 0.002), and incubated an additional 36 h, after which seedlings from each well were removed, quickly dried on paper towels, and transferred to a sterile 2-mL Eppendorf tube. Samples were weighed (to calculate fresh weight) and 400 μL of sterile water plus one 5-mm stainless steel bead was added to each tube. Seedlings were ground with a TissueLyser at 25 shakes per second for 3 min. Aliquots of 100 μL from the ground seedlings were transferred to 96-well plates for light quantification, as desribed above. Enhanced resistance against *X. campestris* pv. *campestris* (*Xcc* strain 33919) was assessed by eliciting seedlings with Flg22 (1 μM) or axY^{s}22-A1 (10 μM) for 24 h and then inoculating with 10 μL of *Xcc* (OD_{600} = 0.002). Bacterial growth was carried out as indicated in *SI Methods*. Seedlings were blotted dry and ground 36 h after inoculation as described above. Serial dilutions were plated on LB agar to determine CFUs.

ACKNOWLEDGMENTS. We thank to J. Bush for plant care. This work was supported by National Institutes of Health Grant R37 GM48707 and National Science Foundation Grant MCB-0519898 (to F.M.A.), National Institutes of Health Grant R01 GM599962 and National Science Foundation Grant MCB-0817738 (to P.C.R.), and by Department of Energy Basic Energy Sciences Grant DE-FG02-02ER15342 (to A.F.B.).

1. Ronald PC, Beutler B (2010) Plant and animal sensors of conserved microbial signatures. *Science* 330:1061–1064.
2. Gomez-Gomez L, Felix G, Boller T (1999) A single locus determines sensitivity to bacterial flagellin in *Arabidopsis thaliana*. *Plant J* 18:277–284.
3. Felix G, Duran JD, Volko S, Boller T (1999) Plants have a sensitive perception system for the most conserved domain of bacterial flagellin. *Plant J* 18:265–276.
4. Asai T, et al. (2002) MAP kinase signalling cascade in *Arabidopsis* innate immunity. *Nature* 415:977–983.
5. Zipfel C, et al. (2004) Bacterial disease resistance in *Arabidopsis* through flagellin perception. *Nature* 428:764–767.
6. Dardick C, Ronald P (2006) Plant and animal pathogen recognition receptors signal through non-RD kinases. *PLoS Pathog* 2:e2.
7. Park CJ, Han SW, Chen X, Ronald PC (2010) Elucidation of XA21-mediated innate immunity. *Cell Microbiol* 12:1017–1025.
8. Song WY, et al. (1995) A receptor kinase-like protein encoded by the rice disease resistance gene, Xa21. *Science* 270:1804–1806.
9. Lee SW, et al. (2009) A type I-secreted, sulfated peptide triggers XA21-mediated innate immunity. *Science* 326:850–853.
10. Lee SW, Han SW, Bartley LE, Ronald PC (2006) From the Academy: Colloquium review. Unique characteristics of *Xanthomonas oryzae* pv. *oryzae* AvrXa21 and implications for plant innate immunity. *Proc Natl Acad Sci USA* 103:18395–18400.
11. Sun W, Dunning FM, Pfund C, Weingarten R, Bent AF (2006) Within-species flagellin polymorphism in *Xanthomonas campestris* pv *campestris* and its impact on elicitation of *Arabidopsis* FLAGELLIN SENSING2-dependent defenses. *Plant Cell* 18:764–779.
12. Millet YA, et al. (2010) Innate immune responses activated in *Arabidopsis* roots by microbe-associated molecular patterns. *Plant Cell* 22:973–990.
13. Songnuan W, et al. (2008) *A Seedling Assay for MAMP Signaling and Infection Studies* (International Society for Molecular Plant-Microbe Interactions, St. Paul, MN).
14. Fan J, Crooks C, Lamb C (2008) High-throughput quantitative luminescence assay of the growth in planta of *Pseudomonas syringae* chromosomally tagged with *Photorhabdus luminescens* luxCDABE. *Plant J* 53:393–399.
15. Bauer Z, Gómez-Gómez L, Boller T, Felix G (2001) Sensitivity of different ecotypes and mutants of *Arabidopsis thaliana* toward the bacterial elicitor flagellin correlates with the presence of receptor-binding sites. *J Biol Chem* 276:45669–45676.
16. Zhang J, et al. (2007) A *Pseudomonas syringae* effector inactivates MAPKs to suppress PAMP-induced immunity in plants. *Cell Host Microbe* 1:175–185.
17. Chinchilla D, et al. (2007) A flagellin-induced complex of the receptor FLS2 and BAK1 initiates plant defence. *Nature* 448:497–500.
18. Denoux C, et al. (2008) Activation of defense response pathways by OGs and Flg22 elicitors in *Arabidopsis* seedlings. *Mol Plant* 1:423–445.
19. Gómez-Gómez L, Boller T (2000) FLS2: An LRR receptor-like kinase involved in the perception of the bacterial elicitor flagellin in *Arabidopsis*. *Mol Cell* 5:1003–1011.
20. Gómez-Gómez L, Bauer Z, Boller T (2001) Both the extracellular leucine-rich repeat domain and the kinase activity of FSL2 are required for flagellin binding and signaling in *Arabidopsis*. *Plant Cell* 13:1155–1163.
21. Dunning FM, Sun W, Jansen KL, Helft L, Bent AF (2007) Identification and mutational analysis of *Arabidopsis* FLS2 leucine-rich repeat domain residues that contribute to flagellin perception. *Plant Cell* 19:3297–3313.
22. Zähringer U, Lindner B, Inamura S, Heine H, Alexander C (2008) TLR2—promiscuous or specific? A critical re-evaluation of a receptor expressing apparent broad specificity. *Immunobiology* 213:205–224.
23. Akira S, Takeda K (2004) Toll-like receptor signalling. *Nat Rev Immunol* 4:499–511.
24. Li J, et al. (2002) BAK1, an *Arabidopsis* LRR receptor-like protein kinase, interacts with BRI1 and modulates brassinosteroid signaling. *Cell* 110:213–222.
25. Shiu SH, et al. (2004) Comparative analysis of the receptor-like kinase family in *Arabidopsis* and rice. *Plant Cell* 16:1220–1234.

Supporting Information

Danna et al. 10.1073/pnas.1106366108

SI Methods

GUS Histochemical Assay. After infiltration of fully expanded leaves of 6-wk-old adult Col-0 wild-type plants with 1 μM Flg22 or Ax21 peptides, plants were kept at 22 °C, 75% humidity, and 100 $\mu E \cdot m^{-2} \cdot s^{-1}$ for 6 h. Infiltrated leaves were transferred to six-well plates containing 5 mL of GUS substrate solution (50 mM sodium phosphate pH7, 10 mM EDTA, 0.5 mM $K_4[Fe(CN)_6]$, 0.5 mM $K_3[Fe(CN)_6]$, 0.5 mM X-Gluc, 0.05% Silwet L-77). Leaves were vacuum-infiltrated for 20 min and then incubated at 37 °C for 4 h. Tissues were fixed with a 3:1 ethanol:acetic acid solution at 4 °C overnight and placed in 95% ethanol. Tissues were cleared in lactic acid and pictures were taken with a Nikon CoolPix 950 digital camera.

Genotyping of T-DNA Insertional Lines. Leaves from 4- to 5-wk-old plants were ground in 2-mL Eppendorf tubes containing 200 μL of DNA extraction buffer (200 mM Tris-HCL pH7.5, 250 mM NaCl, 25 mM EDTA) and one 5-mm stainless steel bead, using a TissueLyser II (Qiagen). After grinding for 3 min at 25 shakes per second, 200 μL of extraction buffer containing 0.5% SDS was added. Samples were briefly mixed and centrifuged at 18,000 × *g* for 5 min. The supernatant was transferred to an empty tube and DNA was precipitated with 1 volume of isopropanol. After 5 min centrifugation at 18,000 × *g* pellets were washed with 1 mL of 70% ethanol. DNA pellets were air-dried and resuspended in 100 μL H_2O. PCR were carried out on 2 μL of template using the primer combinations suggested by SIGnAL (http://signal.salk.edu/tdnaprimers.2.html). A complete list of PCR primers is shown in Table S2.

Mass Spectrometric Analysis of axY^{S}22-A1. Both axY^{S}22-A1 and Flg22 were detected using an Agilent 6520 qTOF LC-MS equipped with a dual electrospray ionization source. Samples were separated using reverse-phase chromatography (C18 extend, 50 × 2.1 mm, 5-μm particle size; Zorbax) at a flow rate of 400 μL/min and a linear gradient of 97% A (water supplemented with 0.1% formic acid) to 10% B (acetonitrile supplemented with 0.1% formic acid) over 1 min and then to 65% B over an additional 6.5 min. Peptides were detected in positive and extended dynamic range (2 GHz) modes between 100 and 3,200 *m/z* using the following instrument settings: gas temperature 325 °C; drying gas (N_2) 10 L/min; nebulizer gas (N_2) 35 psig; fragmentor 200 V; skimmer 65 V; OCT1 Rf Vpp 750 V; Vcap 3500 V; spectra rate 1.02/s, 977.5 ms per spectrum. The *m/z* values were corrected using internal mass references.

qRT-PCR Analysis. Seeds were sterilized in 20% bleach, washed three times with sterile water, and germinated in 12-well microtiter dishes sealed with surgical tape, each well containing 20 seeds and 1 mL seedling growth medium [1× Murashige and Skoog basal medium with vitamins (Phytotechnology Laboratories) containing 0.5 g/L Mes hydrate and 0.5% sucrose at pH 5.7). Seedlings were grown for 10 d at 22 °C in a plant-growth chamber under 16 h of light at a fluence of 100 μE. The medium was changed on day 8. Seedlings were treated with 1 μM Flg22 or 5 μM axY^{S}22-A1 for 3h before RNA extraction. Seedlings were snap-frozen in liquid nitrogen and ground using a mortar and pestle. Total RNA was extracted from 20 seedlings per sample using TRIzol (Invitrogen) according to the manufacturer's instructions. Total RNA was treated with DNase I (Ambion) to avoid genomic DNA contamination, and 2 μg of total RNA was reverse-transcribed using the iScript cDNA synthesis kit from Bio-Rad. cDNAs were purified using the QIAquick PCR Purification Kit from Qiagen. qRT-PCR was performed using a ABI7500 real-time PCR machine (Applied Biosystems) and iQ SYBR Green Supermix (Bio-Rad) using 10 ng cDNA per 20 μL reaction. The program used for qRT-PCR was as follows: 2 min at 50 °C, 10 min at 95 °C, 40 cycles of 15 s at 95 °C/ 1 min at 57 °C. Expression values were normalized to that of the eukaryotic translation initiation factor 4A1 (EIF4A1). Primers used for qRT-PCR were as follows: MYB51_F, 5′-ACAAATGGTCTGCTATAGCT-3′; MYB51_R, 5′-CTTGTGTGTAACTGGATCAA-3′; WRKY53_F, 5′-AAACTGTTGGGCAACGAAAC-3′; WRKY53_R, 5′-AATGGCTGGTTTGACTCTGG-3′; PAD3_F, 5′-TTCCTCTGTTTCCTCGTCCT-3′; PAD3_R, 5′-ATGATGGGAAGCTTCTTTGG-3′; FRK1_F, 5′-ATCTTCGCTTGGAGCTTCTC-3′; FRK1_R, 5′-TGCAGCGCAAGGACTAGAG-3′; PAL1-U1: 5′-AGCCGGTGTGAATGCTAGTAGTG-3′; PAL1-L1: 5′-TGGCTTGTTTCTTTCGTGCTTCC-3′.

Bacterial Growth. *Pseudomonas syringae* pv. *maculicola* strain ES4326 was grown overnight on King's B medium supplemented with Kan at 28 °C and 230 rpm in an orbital shaker, diluted 1:50 dilution in the same medium, grown to OD_{600} = 0.5. Bacteria were centrifuged and washed three times with 1 mL sterile water.

Xanthomonas campestris pv. *campestris* strain 33919 was grown overnight on NYG medium (5 g of peptone, 3 g of yeast extract, and 20 g of glycerol per liter) at 28 °C and 230 rpm in an orbital shaker. Bacteria were grown to OD_{600} = 0.5, centrifuged and washed three times with 1 mL sterile water.

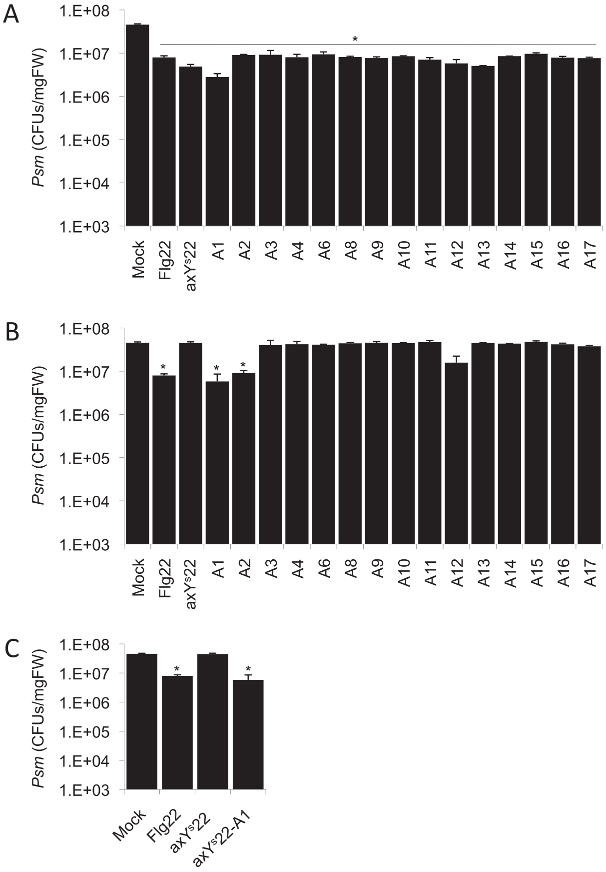

Fig. S1. Activity of axY^{S}22-derived peptides with Ala substitutions. Ten-d-old wild-type Col-0 seedlings grown in 12-well plates were elicited with 100 μM of axY^{S}22-derived peptides or with 1 μM Flg22 (*A*) or 10 μM of axY^{S}22-derived peptides or with 1 μM Flg22 (*B*). A1 to A17 are peptide variants with an Ala substitution at each of the respective positions of the synthetic 17-residue axY^{S}22 peptide (except A1, where the original Ala was replaced by Gly). (*C*) Ten-d-old Col-0 wild-type seedlings were elicited with 10 μM axY^{S}22, 10 μM axY^{S}22-A1 or 1 μM Flg22 for 24 h and the inoculated with *Psm-LUX*. Each column represents the mean ± SD of the bacterial titer 36 h after inoculation from three wells (each one containing 20 seedlings). Essentially identical results were obtained in two independent experiments. *$P < 0.001$ compared with mock (*t* test).

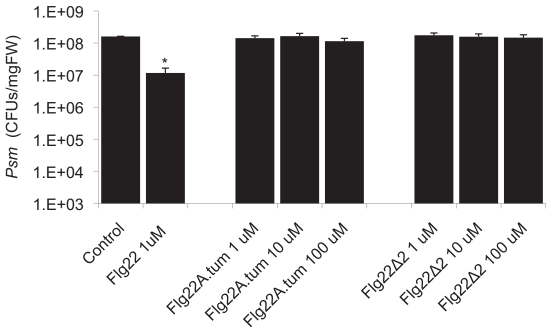

Fig. S2. Inactive peptides are not perceived even at high concentration. Ten-d-old wild-type Col-0 seedlings grown in 12-well plates were elicited with the indicated concentrations of Flg22$^{A.tum}$ or Flg22Δ2 for 24 h and then incoculated with *Psm-LUX*. Bacterial titer was determined 36 h after inoculation. Each column represents the mean ± SD bacterial titer from three wells (each one containing 20 seedlings). Essentially identical results were obtained in three independent experiments. *$P < 0.001$ compared with mock (*t* test).

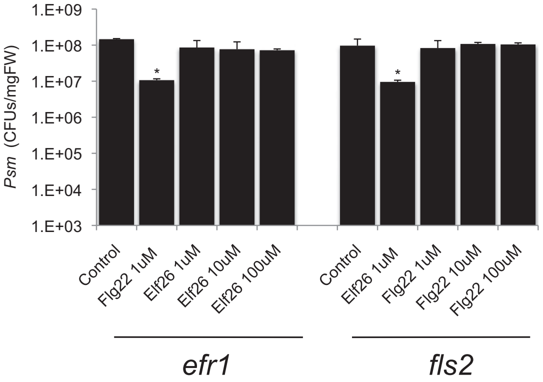

Fig. S3. Active peptides are not perceived in the absence of the cognate receptor even at high concentrations. Ten-d-old *erf1* (SALK_044334) or *fls2* (SAIL_691_C04) mutant seedlings grown in 12-well plates were elicited with the indicated concentrations of Elf26 or Flg22 for 24 h and then inoculated with *Psm-LUX*. Bacterial titer was determined 36 h after inoculation. Each column represents the mean ± SD bacterial titer from three wells (each one containing 20 seedlings). Essentially identical results were obtained in three independent experiments. **P* < 0.001 compared with mock (*t* test).

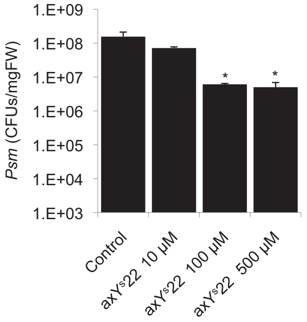

Fig. S4. axYs22 perception is saturable. Ten-d-old wild-type Col-0 seedlings grown in 12-well plates were elicited with the indicated concentrations of axY^{s}22 for 24 h and then inoculated with *Psm-LUX*. Bacterial titer was determined 36 h after inoculation. Each column represents the mean ± SD bacterial titer from three wells (each one containing 20 seedlings). Essentially identical results were obtained in three independent experiments. **P* < 0.001 compared with mock (*t* test).

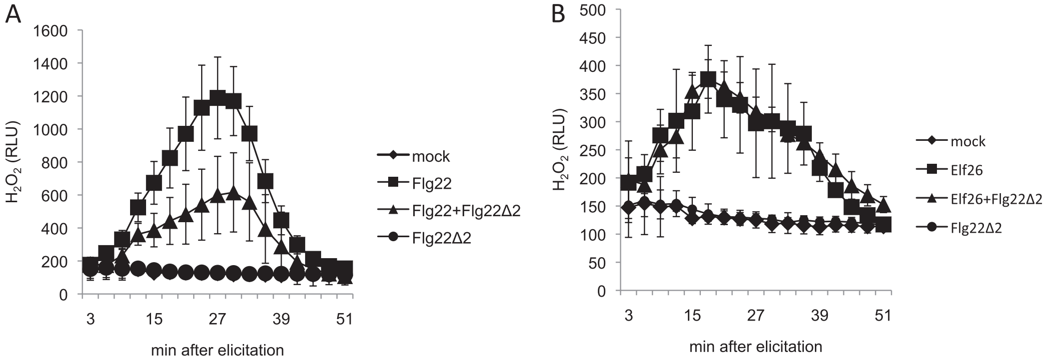

Fig. S5. Flg22Δ2 suppression of Flg22 binding. Chemiluminescence detection of the H_2O_2 burst in 10-d-old wild-type Col-0 seedlings grown in 96-well plates elicited with (*A*) 1 μM Flg22 or 1μM Flg22 + 10 μM Flg22Δ2 or (*B*) 1 μM Elf26 or 1 μM Elf26 + 10 μM Flg22Δ2. Each datapoint represents the mean ± SD of six seedlings (six wells). Identical results have been obtained in at least two independent experiments.

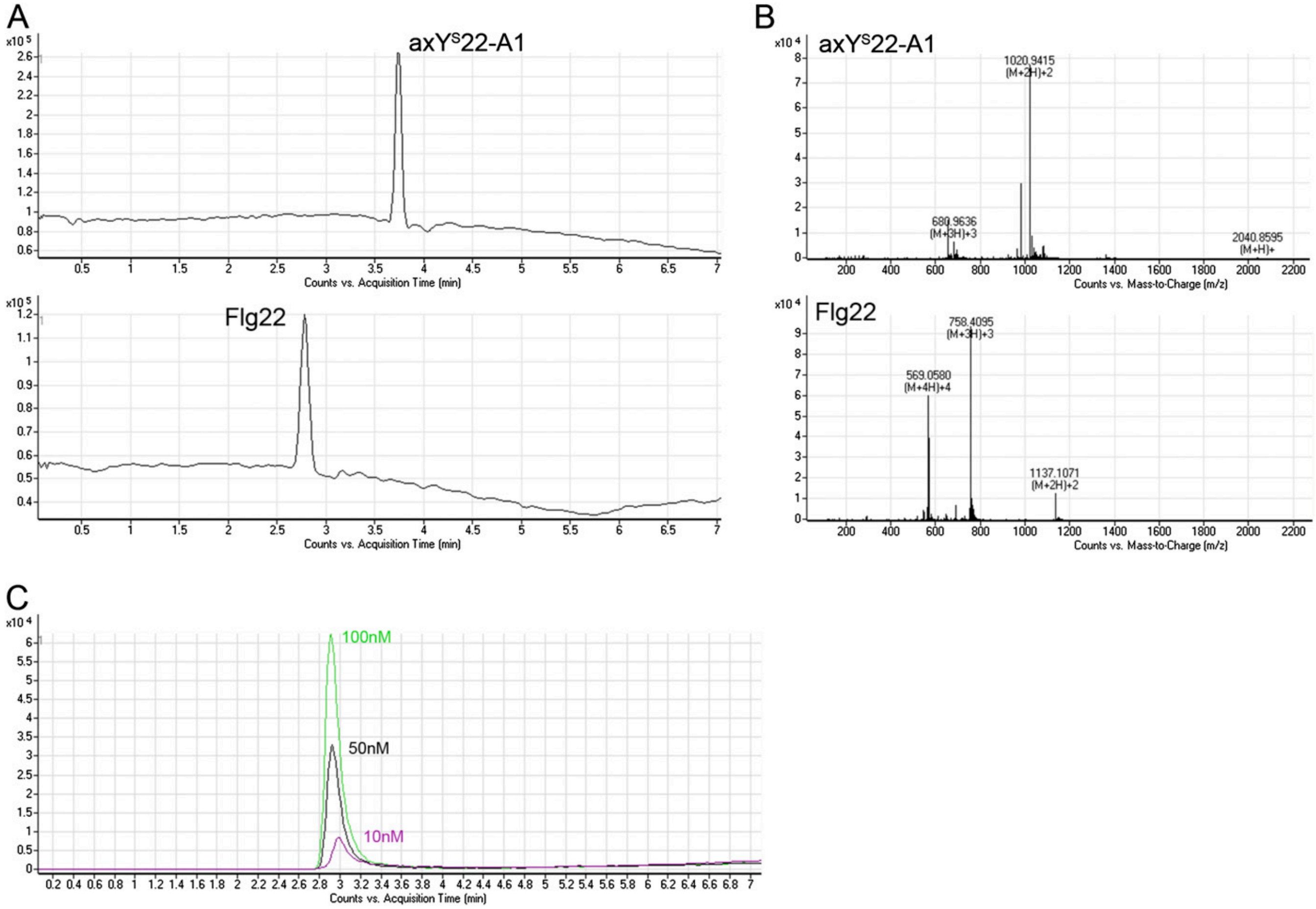

Fig. S6. Detection of axY^{S}22-A1 and Flg22 by mass spectrometry. (*A*) Base peak chromatogram of 10 μM axY^{S}22-A1 and 100 nM Flg22 100 samples (10 μL injection); axY^{S}22-A1 and Flg22 elute at 3.8 and 2.8 min, respectively. (*B*) Corresponding MS spectra for axY^{S}22-A1 (3.714–3.827 min, eight scans) and Flg22 (2.734–2.864 min, nine scans) samples; axY^{S}22-A1 and Flg22 ions are indicated with their corresponding *m/z* and charge. (*C*) Extracted ion chromatogram for 100, 50, and 10 nM Flg22 samples (10-μL injection). The minimal concentration of Flg22 that could be readily detected was 10 nM.

Table S1. List of non-RD IRAK kinase encoding genes, their corresponding T-DNA insertion mutants, and their responsiveness to axY^{S}22-A1 measured as H_2O_2 burst and enhanced resistance against *Psm*

Gene name	Mutant name	T-DNA line	H_2O_2 burst	Enhanced resistance
AT3G09780	*AT3G09780-1*	SALK_089159	Yes	Yes
	AT3G09780-2	SALK_109759	Yes	Yes
AT1G66920	*AT1G66920-1*	SALK_003284	Yes	Yes
	AT1G66920-2	SAIL_563_H08	Yes	Yes
AT1G66930	*AT1G66930-1*	GK-284B09	Yes	Yes
AT1G66980	*AT1G66980-1*	SALK_122292	Yes	Yes
	AT1G66980-2	SALK_139303	Yes	Yes
AT1G67000	*AT1G67000-1*	SAIL_400_A10	Yes	Yes
AT1G70250	*AT1G70250-1*	SAIL_125_D06	Yes	Yes
AT4G18250	*AT4G18250-1*	SALK_056431	Yes	Yes
	AT4G18250-2	SALK_036670	Yes	Yes
AT5G38240-	*AT5G38240-1*	SALK_142662	Yes	Yes
AT5G38250	*AT5G38250-1*	SAIL_670_C08	Yes	Yes
AT5G38260	*AT5G38260-1*	SAIL_316_B08	Yes	Yes
	AT5G38260-2	SALK_049448	Yes	Yes
AT5G38280	*AT5G38280-1*	GK-254G07	Yes	Yes
AT5G39020	*AT5G39020-1*	SALK_125986	Yes	Yes
	AT5G39020-2	SALK_122162	Yes	Yes
AT5G39030	*AT5G39030-1*	SALK_007613	Yes	Yes
	AT5G39030-2	SALK_014892	Yes	Yes
AT2G13800	*AT2G13800-1*	SALK_147275	Yes	Yes
AT1G68400	*AT1G68400-1*	GK-218D01	Yes	Yes
AT5G05160	*AT5G05160-1*	SALK_056624	Yes	Yes
	AT5G05160-2	SALK_074276	Yes	Yes
AT1G80870	*AT1G80870-1*	SALK_049258	Yes	Yes
	AT1G80870-2	SALK_138934	Yes	Yes
AT4G26540	*AT4G26540-1*	SALK_053167	Yes	Yes
	AT4G26540-2	SAIL_1220_B03	Yes	Yes
AT5G56040	*AT5G56040-1*	SALK_052069	Yes	Yes
AT2G24130	*AT2G24130-1*	SALK_025037	Yes	Yes
	AT2G24130-2	SALK_101008	Yes	Yes
AT3G47090	*AT3G47090-1*	SALK_101474	Yes	Yes
	AT3G47090-2	SALK_026298	Yes	Yes
AT3G47110	*AT3G47110-1*	SALK_101668	Yes	Yes
	AT3G47110-2	GK-182H05	Yes	Yes
AT3G47570	*AT3G47570-1*	SALK_063487	Yes	Yes
	AT3G47570-2	GK-415H04	Yes	Yes
AT3G47580	*AT3G47580-1*	SAIL_252_H12	Yes	Yes
AT5G20480	*AT5G20480-1*	SALK_044334	Yes	Yes
	AT5G20480-2	SALK_068675	Yes	Yes
AT5G39390	*AT5G39390-1*	GK-026A08	Yes	Yes
	AT5G39390-2	SAIL_1162_B02	Yes	Yes
AT5G46330	*AT5G46330-1*	SAIL_691_C04	No	No
	AT5G46330-2	SALK_141277	No	No
AT3G26700	*AT3G26700-1*	SALK_142166	Yes	Yes
AT2G45910	*AT2G45910-1*	GK-122F04	Yes	Yes
AT2G30940	*AT2G30940-1*	SALK_137752	Yes	Yes
AT5G18910	*AT5G18910-1*	SALK_129579	Yes	Yes
AT2G45590	*AT2G45590-1*	SALK_087417	Yes	Yes
AT4G25390	*AT4G25390-1*	SALK_093369	Yes	Yes
AT5G51770	*AT5G51770-1*	SALK_056450	Yes	Yes
	AT5G51770-2	SALK_075797	Yes	Yes
AT1G33260	*AT1G33260-1*	SALK_049165	Yes	Yes
AT4G10390	*AT4G10390-1*	GK-658A06	Yes	Yes
AT1G52540	*AT1G52540-1*	SALK_016081	Yes	Yes
AT3G15890	*AT3G15890-1*	SALK_085834	Yes	Yes
AT5G20050	*AT5G20050-1*	SALK_000490	Yes	Yes
AT1G34300	*AT1G34300-1*	SALK_132270	Yes	Yes
	AT1G34300-2	SALK_147692	Yes	Yes
AT2G19130	*AT2G19130-1*	SALK_000051	Yes	Yes
	AT2G19130-2	SALK_118926	Yes	Yes
AT4G00340	*AT4G00340-1*	SALK_116983	Yes	Yes

Table S1. Cont.

Gene name	Mutant name	T-DNA line	H_2O_2 burst	Enhanced resistance
AT4G32300	*AT4G32300-1*	SALK_105027	Yes	Yes
	AT4G32300-2	SALK_076638	Yes	Yes
AT5G35370	*AT5G35370-1*	SALK_123639	Yes	Yes
	AT5G35370-2	SALK_024084	Yes	Yes
AT5G60900	*AT5G60900-1*	SALK_084958	Yes	Yes
	AT5G60900-2	SALK_146547	Yes	Yes
AT1G66910	*AT1G66910-1*	WISC_145_096	Yes	Yes
AT5G24080	*AT5G24080-1*	SAIL_551_D12	Yes	Yes
	AT5G24080-2	SALK_147104	Yes	Yes

The 12 genes encoding cytosolic non-RD IRAK kinases are shown in bold. The remaining 35 genes encode non-RD IRAK RLKs.

Table S2. List of non-RD IRAK kinase encoding genes, their corresponding T-DNA insertion mutants, and primers used for the identification of homozygous plants through PCR genotyping on genomic DNA

Mutant name	T-DNA line	Left primer	Right primer
AT3G09780-1	SALK_089159	TTCTGGTGATGGGTTTAGCTG	AAACCCACTGTGCAGATGATC
AT3G09780-2	SALK_109759	TTCTGGTGATGGGTTTAGCTG	TTGTGTGGATTATGGTTGCTG
AT1G66920-1	SALK_003284	GAAACAAAATGCAAGTGGACC	CTTGAAGCACAAGGAAGATGG
AT1G66920-2	SAIL_563_H08	AATCCTTGTTCTGCAACCATG	CACTCTACCGTTGCTACCCTG
AT1G66930-1	GK-284B09	TTATTCCACCCTCTTCCTTGG	TCTTCCCTCATCACAACCAAG
AT1G66980-1	SALK_122292	GGGTACAAGAATCCCTGAAGC	AATTCCCAGCAAAGTACTCGG
AT1G66980-2	SALK_139303	TTGTTTTGTAGCGTTTCTGCC	AGCCGATGTTGTTCTATGGTG
AT1G67000-1	SAIL_400_A10	TGACCAGAGTCGCTGTAAACC	TTTCTGTTCCTTGCCACTTTG
AT1G70250-1	SAIL_125_D06	GAGTTTTGTGGAAGCAAGTGG	TATACCTGGAGGTGGAGGGAG
AT4G18250-1	SALK_056431	TGGATTTACATTTCAAACCGC	GGGCAACGAAAAGAGAAGAAG
AT4G18250-2	SALK_036670	CTATGAAGGGAGCCAGAGAGC	TTGGAGCGAGCATTTAATCAC
AT5G38240-1	SALK_142662	CAAGAAAGAGGCAATTTGCAC	CGGTCGTTTTGACTTCAAGAG
AT5G38250-1	SAIL_670_C08	CATATGAGACGTTGGGGAATG	GCAAAGGTGTGGAAGAGAATG
AT5G38260-1	SAIL_316_B08	ACGGTAATAAGAGTGGCACCC	TGAACTGGACAAACAATTCGTC
AT5G38260-2	SALK_049448	CCGCCTATTTTGACAGCTCTAC	TTGTTTGTCCAGTTCACGATG
AT5G38280-1	GK-254G07	GTTCCAAATCCTCCTTTACCG	TCGTGGATGGTTACAACCTTC
AT5G39020-1	SALK_125986	GCAACATCATAAAGAACAACCC	TAGCATACACATCATACGGCG
AT5G39020-2	SALK_122162	CTATCTGGAAGTCAACGTCGC	TGAAACTTCATAGGTCTGCGG
AT5G39030-1	SALK_007613	GACTTGCATCCTCTGGTGAAG	TCCTTCCATCATTTCAACGAC
AT5G39030-2	SALK_014892	GCATCGACTGTAAAGAGCCAG	ATGATTGGTACGTTGGAGCTG
AT2G13800-1	SALK_147275	GATGAGCTCGAGAAGCATGAC	AACATTCCACTTGGTTGATGC
AT1G68400-1	GK-218D01	ACCATGGAGAAGCCAGAAGAG	CAAACCTCTCGAACCTCACAG
AT5G05160-1	SALK_056624	CCCTCCTTTCTTTACGGTGTC	CTGCGGTTTCTTGCTATTCAC
AT5G05160-2	SALK_074276	AAACTTTTGGTCGGAATGAGG	GTGAATAGCAAGAAACCGCAG
AT1G80870-1	SALK_049258	GATGCTCTTCCTCTTTCCACC	TGTGATTGGTAAAGGTGGCTC
AT1G80870-2	SALK_138934	TTTTCATGCCACATTTCAAGG	AGGAATATGGAGGAATGGTGG
AT4G26540-1	SALK_053167	TTTACAATCCCAACGCACTTC	CGTGCAATTCGTTAGCTCTTC
AT4G26540-2	SAIL_1220_B03	AAAGCCTCGAGTTTCTCGATC	ATTCCGGTATTTGGATAACCG
AT5G56040-1	SALK_052069	TTCCAGTTCCGATCACGTTAG	GTCAAGAGCTTCAAGCGATTG
AT2G24130-1	SALK_025037	TATGGAACTCGGGGATATTCC	GCAGAACAAGAGCGTTGAAAC
AT2G24130-2	SALK_101008	ACAGTACCGGTGAGCTTGTTG	CACATCGGACATTGTTGAGG
AT3G47090-1	SALK_101474	TAGGCATTTTGCAATTGCTTC	TGCAAATGGGAGCAATTAGTC
AT3G47090-2	SALK_026298	ATTTCCAAGAGAGGTTGGGAG	CAGCTGGAAGTGGGTTAGATG
AT3G47110-1	SALK_101668	TTGGGAAACCTGACATCACTC	CCGTCGAAGTTGTTCAAAGAG
AT3G47110-2	GK-182H05	CACGTCTCCCATAATTGATGG	CTTTGAACAACTTCGACGGAG
AT3G47570-1	SALK_063487	AGAAAAACATACCCATTCCCG	ATGCTTCTCATGTTTTGCAGG
AT3G47570-2	GK-415H04	ATGCTTCTTCACCACAGATGG	GGAGGGAATTATTTCACAGGG
AT3G47580-1	SAIL_252_H12	CTGTCTGATAACGCTTTTGGG	AGAGCCGCTCAAAGAGTTACC
AT5G20480-1	SALK_044334	TTGCCAATATCTCAAGCCTTG	AAACACTCCTGTTGTTGGCAC
AT5G39390-1	GK-026A08	GGAATGCTATTTAGGCTTCGG	ACCAAATGAATTGTCTGTCGG
AT5G39390-2	SAIL_1162_B02	TTTGAAAGATTCACATTCCGC	GCAAATTGCTTTCTTGGTGAC
AT5G46330-1	SAIL_691_C04	ACATGTCCGGTACTATCGCAG	TCCATCAAGACAGCTAATGAGC
AT5G46330-2	SALK_141277	AGGGCTTCTTACAAACCTTCG	CGTTGATGTTTTTGAACACCC
AT3G26700-1	SALK_142166	CAGGACACAAGCTAGAGCTGG	TTAATCGCCGATGAAGTTGAG
AT2G45910-1	GK-122F04	GCATAGTGCACTTGTTCGTCTC	CTTCTTGCCTCCAGTGTTTTG
AT2G45910-2	SALK_125263	GTTCTCACACTTTTGCTTCCG	CACTTGGAGAGATCCCTAGGC
AT2G30940-1	SALK_137752	CTGAGCCTTCTGTATTGCCTG	TGTCAAACGATTCCTTCCAAG
AT5G18910-1	SALK_129579	AAGCAGGACGGAGAAGATAGC	TTGATCCGATTCTGGAAGATG
AT2G45590-1	SALK_087417	CGGAGATCTTTGCAGACAAAG	CTTGAGGAGACTGAAAGCGTG
AT4G25390-1	SALK_093369	TACCACTACCACTACCACGCC	GAATAGACTAGGTCAGGGCGG
AT5G51770-1	SALK_056450	GATTCACTGATCAGTCTCCGG	ATCTACCACCAAAGAAACCGC
AT5G51770-2	SALK_075797	TTCTCCGCTTCTTCTTCTTCC	ACCTCACCATGAAACAACCAC
AT1G33260-1	SALK_049165	AACCGGTTACCGAATTTCATC	GCTTTTCCTTGTTGCAAATTG
AT4G10390-1	GK-658A06	GCTACTGATACAGACCGCAGC	CTTTGCTTTGCTCTGTTCTGC
AT1G52540-1	SALK_016081	GGACCTGTTTTGGTTAAAGGC	ATACACACTGCCAAATCTGCC
AT3G15890-1	SALK_085834	TCCTTTGATTCATTCACCAGC	TAACAAACTCGGTGAAGGTCG
AT5G20050-1	SALK_000490	TTCGGGTTTAACATCGAGATG	AATCCAACTTGGCACAACTTG
AT1G34300-1	SALK_132270	CTTTCGAGTTGTTATCGTCGC	CCTTCCCCTAACTCCTTCCTC
AT1G34300-2	SALK_147692	CCCAGTAAAGAAGGAACCAGG	GCCATTTCTCAAACTTCTCCC
AT2G19130-1	SALK_000051	ACCGGAGTCTGGTAATTACCG	TCATTTACGGCGAATCAAAAG
AT2G19130-2	SALK_118926	GCTCTTTCCGGTTCGTTTATC	TCAAAACGATTTTGTAACGTGG
AT4G00340-1	SALK_116983	ATCCGTCGCTGTAATCATCAG	TTTTAGTTCCTATCCTGCCGG

Table S2. Cont.

Mutant name	T-DNA line	Left primer	Right primer
AT4G32300-1	SALK_105027	TCCATCTTTGAATTCCACCTG	TCAAAGATGATGAAATTCCGG
AT4G32300-2	SALK_076638	CTGCTCGGGTTCTAAAGTGTG	ATTCTGGAGCCAAGTAGCCTC
AT5G35370-1	SALK_123639	GATTCTCCGGGAAGAATCTTG	TATGATCTTCTGGTCGCAACC
AT5G35370-2	SALK_024084	GATTCTCCGGGAAGAATCTTG	TTAGGTTGGAAATGATCGTGC
AT5G60900-1	SALK_084958	TCACACCTTCAAGCATCTGTG	CTCACGGTGAAAGATCTCCAC
AT5G60900-2	SALK_146547	TTTTGACAAAATTGCAAACGC	TTGTTCCAAAAATAACCGCAG
AT1G66910-1	WISC_145_096	TGACTAAATCCACAAGCACCC	GTAATCTTTGCGGAAAGGAGC
AT5G24080-1	SAIL_551_D12	CAAGGTTCATGTGATGCATTG	ACATCAATCTTGACCCTCACG
AT5G24080-2	SALK_147104	AGAGCATTCGCATGTGGTTAC	GAAACGCTCTCATGGAAGTTG